Applications of Fracture Mechanics to Quantitative Accelerated Life Testing of Plastic Encapsulated Microelectronics

John W. Evans

NASA HQ, Office of Safety and Mission Assurance

Koustav Sinha

CALCE Center

University of Maryland

Accelerated testing must address the failure mechanisms active within the devices undergoing tests in order to assess lifetimes in a meaningful way. The assumption of constant temperature, thermally activated lifetime, based upon the Arrhenius assumptions, does not always provide the necessary understanding to interpret accelerated tests in microelectronics. Plastic encapsulants, dielectric polymers, and underfill materials are subject to delamination and cracking with thermal cycling. Crack propagation during use environment exposure, drives the potential for failure of microelectronic devices and is therefore a necessary focal point in qualification and life testing. This paper reviews the available research in the application of fracture mechanics to this class of problems in microelectronics including relevant test data. In addition, useful acceleration factor models are derived for polymer crack propagation based on principles of linear elastic fracture mechanics. Further, a simple approach to estimating the minimum temperature cycling ranges, necessary to propagate a crack, is also presented. Finally, a methodology of applying acceleration factors to develop testing plans is shown, with an example in spaceflight for a cubesat in low Earth orbit. Overall, this is a paper that shows a useful and appropriate process for creating physics of failure based life testing for delamination and cracking failures in microelectronic polymers in a temperature cycling environment.

Introduction

Polymers play a crucial role in enabling modern microelectronic devices, from encapsulating simple diodes to the most complex digital processors. Polymers are a mainstay of modern microelectronic packaging [1, 2]. These materials perform the crucial function of providing structural enclosures that protect the active silicon element from the environment, while enabling handling and interconnection of the devices for assembly into functional circuits. The mechanical and dielectric properties of polymer materials, along with the range of economic options in processing, are what make them so important to the microelectronic industry. As shown in Figure 1, an advanced device will encompass a number of layers of materials and interfaces within the structure. Adhesion and integrity of the polymer system is critical to the reliability of these devices [1]. Due to mismatches in properties and contact morphology these material interfaces are vulnerable to failure through delamination and crack growth under various loading patterns. The crack initiation and growth rate follows the theories of fracture mechanics which can be used to directly understand the durability of the system. These principles are subsequently explained along with useful applications to testing of microelectronic devices that depend on polymer packaging.

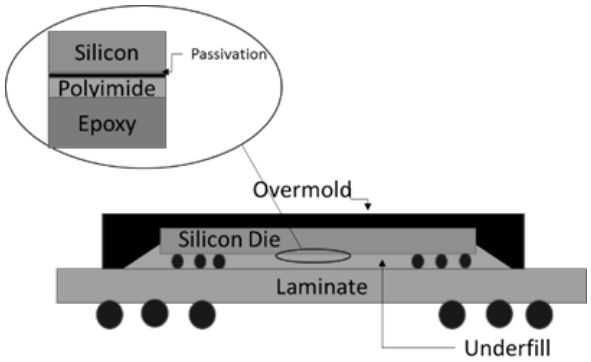

Figure 1: Simplified schematic of over molded flip chip ball grid array. The inset shows typically layered structure on which the reliability of these devices depend.

Function and Properties of Microelectronic Polymers

The major classes of polymers used in microelectronic packaging include epoxies and polyimides. For many types of advanced devices, polyimides are applied, as a film, over the hard layers of inorganic passivation, as one of the last steps in fabrication of the wafer. This application provides for defense of the active circuits on the surface of the die, against subsequent handling. This enables packaging and allows for the assembly of the silicon device into useful products, similar to the structure shown in Figure 1. In addition, polyimide provides for a barrier against moisture during handling, packaging and service. Polyimide films also reduce stresses imparted to the surface of the circuits by the surrounding encapsulations that make up the package structure. Variations in polymer chemistry which make up this class of polymer (polyimides) will not be discussed in detail, but it is important to note specific polymer compositions may have specific responses to loading and environment, given different thermal and mechanical properties that are a result of the chemical variations in the polymeric chains [2, 3].

Polyimide chemistry can be made to be photoimageable. This combined with superior dielectric properties, and thermal stability, enable high yield processing that is key to cost effective advanced devices. Polyimide is preferred for advanced packaging applications such as the addition of solder bumps for flip chip. They are also used in many other types of devices including high voltage applications, PIN diodes and microelectromechanical systems (MEMS), owing to processability, mechanical and dielectric compatibility, and thermal stability.

Epoxies are also highly versatile and diverse in terms of composition, properties and processing, enabling their use for structural functions and final packaging or encapsulation. Epoxy based *adhesives* are used for structural bonding, including die attach for conventional wirebond devices, as well as underfill for advanced flip chip devices. Figure 1 shows a typical high volume, high input-ouput (IO) pin count package schematic common in microelectronics. This is an example of an encapsulated device in which interface adhesion plays a critical role in the reliability of the device. There are many other devices types ranging from optocouplers to MEMS that depend on polymer integrity to ensure reliability.

Die bond applications for epoxy adhesives are well understood, as this has been a mainstay of packaging for many years. However, development of flip chip has driven the need for improvement in understanding of reliability considerations for epoxies used in underfill applications. In the case of adhesives, pre-formed

solids or liquid applications are used. For advanced flip chip devices, underfills are often applied in liquid applications which depend on capillary action to fill the gap between the device and chip carrier [2]. Filling the gap reduces the opportunity for moisture to reach the active surface of the die and provides for the structural integrity that relieves plastic strain in the solder joints.

The properties of epoxy adhesives and liquids are modified with fillers to provide control of thermal expansion properties. A variety of particulate fillers can be used to control thermal expansion to more closely match other components in the package structure. This is the key to providing reduction and control of stress, given differences in thermal expansion between the die and the chip carrier. For many types of devices, printed circuit board laminates are preferred for cost considerations, but ceramics are also employed for specialty applications.

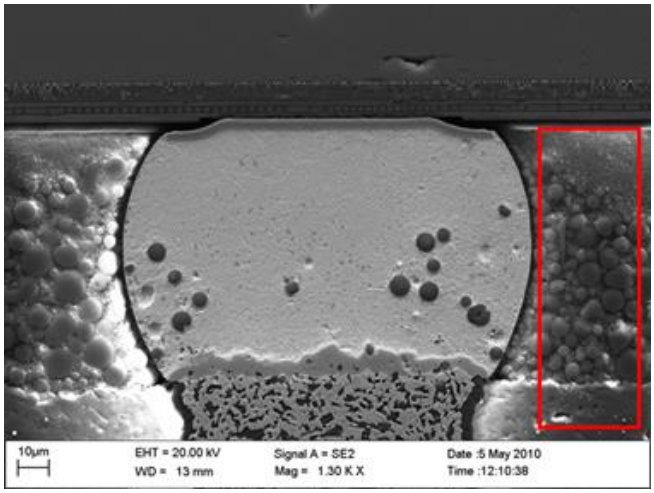

Figure 2: Solder bump electron micrograph showing the bump and surrounding epoxy underfill. The inset shows the epoxy matrix heavily loaded with particulate fillers to control thermal expansion of the matrix. (Courtesy of J.O. Suh, NASA JPL.)

Figure 2 shows a solder bump section revealing the adjacent underfill that is heavily loaded with particulate fillers for control of thermal expansion of the epoxy matrix. Fillers may also be used to impart electrical conductivity or to enhance thermal conductivity. These fillers also affect the mechanical behavior including fracture as the crack tip interacts with the particulates.

Epoxy *molding compounds* are most often used for final packaging of advanced devices but liquid applications are also used for a variety of applications for final encapsulation (glob-top). Transfer molding is often used to facilitate rapid processing and yield. The composition of molding compounds or encapsulants can be substantially different from adhesives, but fillers are also commonly used to control their properties.

Failures in Polymer Packaging

The system of materials in the realm of modern polymer encapsulated packages creates complex multilayer structures. The reliability and lifetime for these devices depends on the integrity of these multilayer polymer structures. However, failures and defects can and do occur in application and testing.

Delamination or failure of a bonded interface is a primary failure mechanism of packaged structures. Therefore, adhesion of the layers in structure is critical to the reliability of many classes of semiconductor devices. *Delamination precedes other failure mechanisms in microelectronic devices*, which activate as a result of loss of the functions that polymers provide in the devices. Delamination will generally mean a loss of the dielectric or electrical insulating function, loss of structural integrity and stress control and a loss of the moisture barrier. Hence, for flip chip devices, delamination precedes corrosion of circuit elements and fatigue of the solder bumps [1, 4, 5]. An example of failure of underfill in an unencapsulated flip chip device, assembled to a ceramic substrate and employing an epoxy underfill, is shown in Figure 3. The micrograph prominently shows the fillet loss. However, the propagation of the crack along the epoxy to chip carrier interface in this device is of greater concern, as the propagation of the crack will increase the likelihood of solder bump failure with the loss of structural integrity afforded by the underfill.

Cracking within the polymers, as well as along interfaces, is also a failure mode of concern. For example, cracking of polyimide passivation will cause a loss of the passivation protection it affords the die [6] leading to electrical leakage currents and corrosion. In the case of some types of high voltage devices, this will precede a catastrophic electrical failure. Passivation cracking in a polyimide coated die stack is shown in Figure 4.

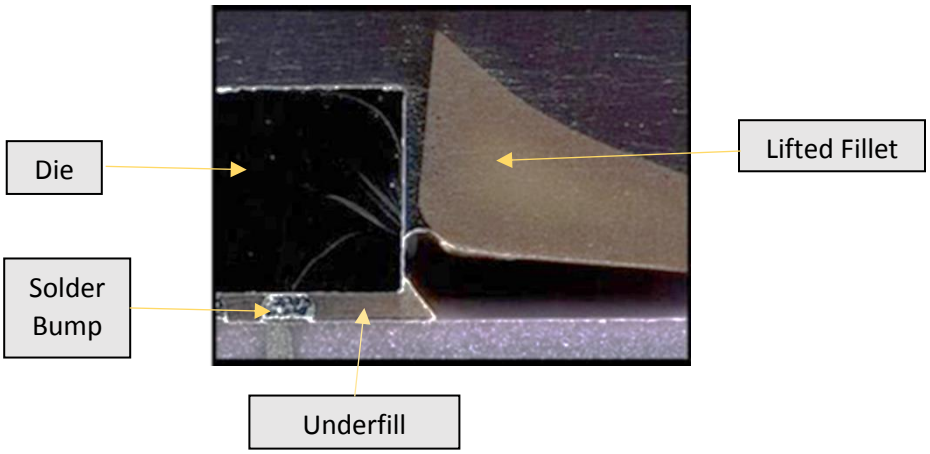

Figure 3: Unencapsulated flip chip structure with failed underfill. (Courtesy of Scott Popelar, Cobham Semiconductor Solutions (formerly Aeroflex))

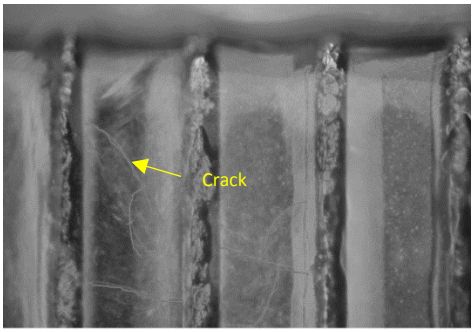

Figure 4: Cracking in a polyimide passivation on a die stack. Cracks are decorated to enhance visualization. (Courtesy of Ahmed Amin and Henning Leidecker NASA GSFC.)

Thermal stresses are predominant in driving failure in polymer encapsulated electronics. Thermal stresses arise from differences in the coefficients of thermal expansion (CTE) of the materials and the changes in temperature that occur from use environments and operation of the devices. A typical portion of an underfill is depicted in Figure 5. The difference in the thermal expansion between the epoxy underfill and the silicon die can easily exceed 10 to 15 ppm/^{o}C depending on the amount of fillers in the epoxy and the specific epoxy composition, structure and processing.

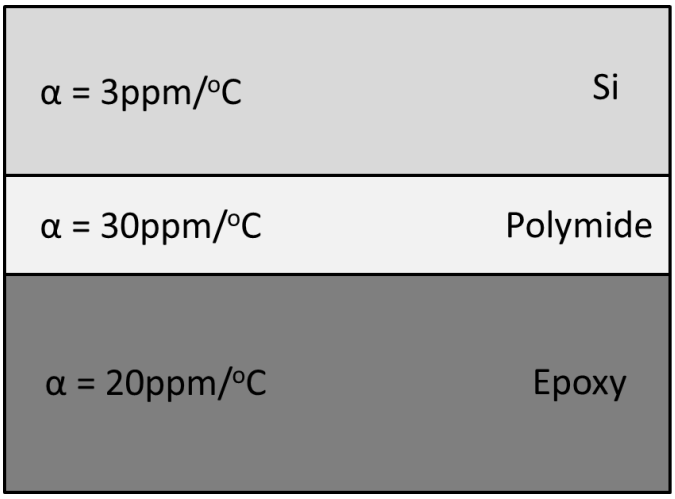

Figure 5: Multilayer structure with typical coefficients of expansion.

In simplest terms, the stress range developed in any particular material that is part of any stacked structure similar to Figure 5, are expressed in equation 1. They are proportional to the effective modulus of elasticity, $\bar{E} = {}^{E}/_{1-\nu}$, where E is the Young's modulus of the material and ν is the Poisson ratio, as well as the differences in CTE, $\Delta\alpha$, of the materials in the structure and the temperature changes, ΔT, that the structure experiences.

$$\Delta S = \bar{E}\Delta\alpha\Delta T \qquad (1)$$

The mechanically stiffer elements drive the forces developed in the individual materials, as determined by the modulus of elasticity and thickness. When the system is not symmetrical, bending stresses will tend to develop, introducing additional complexity. Approximate closed form solutions to stresses in a multilayer structure are given by Suhir [35, 36]. The actual state of stresses in a multilayered structure may be complex and material properties can be dependent on temperature and time, as well. Detailed analysis of a microelectronic package are often best handled in carefully prepared finite element models (this topic will not be further developed and reader is referred to the references) [6].

Elements of Fracture Mechanics for Polymers

Linear Elastic Fracture Mechanics (LEFM) has been widely applied to polymers to describe the growth of cracks in cyclic loading of laminates [7] and in studying materials that comprise microelectronics interfaces [8, 9, 10, 11 and 12]. Some basic elements of LEFM are explained below as necessary for understanding application to accelerated testing of microelectronic devices.

In general, crack growth may occur in three specific fundamental modes. The opening mode or Mode I occurs under tensile loading in which the opposing faces of the crack are separated with application of the load, as reflected in Figure 6. In general, it takes less energy to propagate a crack in Mode I than in other modes. Mode II growth is also known as the edge sliding mode. This occurs in shear and is often associated with cracking in microelectronic type structures, under thermal cycling or vibration loads. The third mode, Mode III, also occurs in shear and is known as the tearing mode.

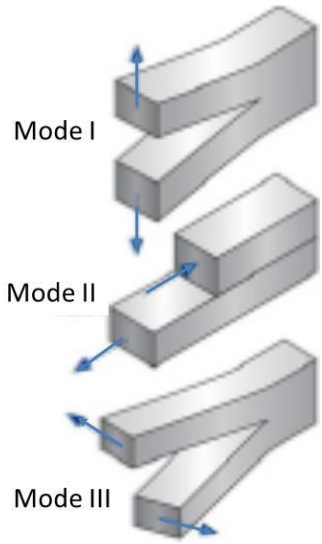

Figure 6: Primary modes of crack growth.

Crack growth in polymers used in microelectronics becomes a complex process of mixed modes of loading and crack growth. While shear loading apparently dominates, structures are rarely symmetrical, which leads to mixed modes of loading and crack growth, combining shear and tensile loading. Tensile loading develops as a result of some bending that will occur in non-symmetrical stacked structures of materials with different coefficients of thermal expansion (CTE) of the type shown in Figure 5 [8].

The basics of crack development in polymers differs from metals. Even in shear dominated loading, crack tip behavior in polymers is dominated by tensile behavior and tensile fracture properties; hence, Mode I material properties are most the important in describing failure [7, 13]. This is due to the formation of secondary microcracks at the forefront of the primary crack tip. In Mode II loading of polymers, these secondary cracks are near an angle of 45^0 to the fracture surfaces of the primary opening crack. This clearly shows the dominance of tensile behavior, as this orientation reflects the influence of the principal stresses. *Ligaments* form between the secondary cracks, in front of the primary crack, and subsequently rupture under continuous loading. The coalescence of rupturing ligaments forms new primary crack surfaces.

At the interface between two different polymers, such as polyimide and epoxy, crack propagation occurs adjacent to or within an interfacial or interphase layer that forms as a result of bonding the two polymers [5]. Failure does not necessarily occur with a clean separation of two separate materials in a properly formed bond. Snodgrass [9] showed that cyclic growth of cracks in the epoxy-polyimide systems, for example, favored crack growth along the interface in the epoxy side of the bond, through formation of ligaments in the epoxy.

These fundamentals of polymer mechanics are clearly not dependent upon sliding surfaces in Mode II in the classical sense of LEFM. It is the premise of this paper, therefore, that tensile properties, which are easily measured, can be used to provide for information to formulate accelerated test designs, when evaluating complex layers of polymers in microelectronic structures.

Theoretical Foundations - Derivation of Fracture Parameters

Prediction of interfacial failure in an accurate manner is heavily dependent on appropriately determining the stress intensity factors or strain energy release rate, whichever is more appropriate for the particular case. These interfacial properties are more dependent on bonding/fabrication process conditions unlike homogeneous materials. This makes specific tests necessary to determine the interfacial fracture parameters, which are then derived through load-displacement measurements and applied to theoretical models.

Stresses attain their highest value at the corner edge of a multimaterial junction in electronic packages. High stresses and inherent bond weakness due to manufacturing defects can result in crack initiations at the corners. One such region of great concern is the bond between silicon die and flip chip underfill material (reinforced polymer). Sharp three dimensional corners completely embedded in polymer are locations of highest stress in the package under thermomchanical loading.

Fracture theories have their roots in elasticity solutions where stress singularities take the form

$$\sigma_{ij} \propto r_D^{-\lambda} \qquad (2)$$

where r_D is the radial distance from the corner to the point at which stress is measured. The power index, λ, independent of the loading conditions, is a complex number and can be expressed as follows [14]:

$$\lambda = \gamma + i\eta \qquad (3)$$

where γ and η are the real and imaginary components respectively. The consequence of λ being a complex number is the stress state becomes oscillatory in nature. For stress state inside the nonlinear fracture process zone close to the crack tip can be solved by letting $\alpha_1 = +\pi$ and $\alpha_2 = -\pi$ [15] in Fig. 7 which is asymptotic in nature and can be expressed in the form

$$\sigma_{ij} = \frac{1}{\sqrt{2\pi r_D}} \{\mathrm{Re}[K r_D^{i\varepsilon}]\tilde{\sigma}_{ij}^{I}(\theta,\varepsilon) + \mathrm{Im}[K r_D^{i\varepsilon}]\tilde{\sigma}_{ij}^{II}(\theta,\varepsilon) + K_{III}\tilde{\sigma}_{ij}^{III}(\theta,\varepsilon) \qquad (4)$$

where r_D and θ are the local polar coordinates for a coordinate system in planes perpendicular to the crack front.

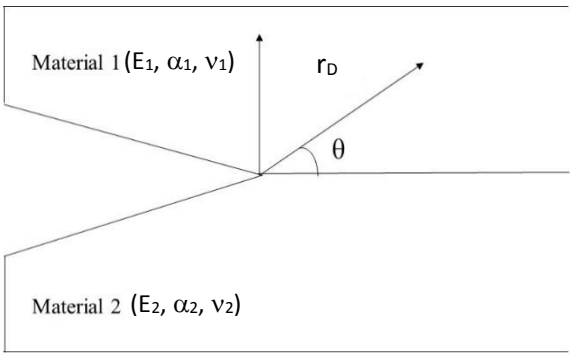

Figure 7: Local coordinates (r_D, ϑ) for asymptotic interface crack solutions

The stress in eqn (4) comes from the complex exponent of r that can be expressed as

$$r^{i\varepsilon} = \cos(\varepsilon \ln r_D) + i\sin(\varepsilon \ln r_D) \qquad (5)$$

The stress intensity factor K has real and imaginary parts K_I and K_{II} ($K = K_I + K_{II}$) that are similar to the conventional Mode I and Mode II stress intensity factors in homogenous materials. For interfacial problems, K_I and K_{II} are dependent on each other and only the Mode III behavior is independent. The imaginary power $r^{i\varepsilon}$ depends on the oscillatory index ε as follows:

$$\varepsilon = \frac{1}{2\pi} \ln\left[\frac{1-\beta}{1+\beta}\right] \qquad (6)$$

β here is knowns as one of the two Dundur's parameters. Dundur's parameters are unitless quantities defining the elastic mismatch and can be defined by-

$$\alpha = \frac{\mu_1(k_2+1) - \mu_2(k_2+1)}{\mu_2(k_1+1) + \mu_1(k_2+1)} \qquad (7)$$

$$\beta = \frac{\mu_1(k_2-1) - \mu_2(k_2-1)}{\mu_2(k_1+1) + \mu_1(k_2+1)} \qquad (8)$$

where μ is the shear modulus, κ= 3-4ν for plane strain or κ= (3-ν)/(1+ν) for plane stress (ν is Poisson's ratio). The subscripts 1 and 2 depict the two different materials on the two sides of the universe.

So let's now look at an example of a bimaterial interface of epoxy polymer and silicon interface which is a common failure site in electronic packages. Using their standard elastic properties of Silicon (E = 128.3 GPa, ν = 0.28) and Epoxy (E = 12.0 GPa, ν = 0.33) and incorporating them in eqns. (7), (8) and (9) we can calculate the Dundur's parameters as α = 0.8235, β = 0.2044 and a relatively large oscillatory index of ε = -0.066. At that level of ε, there is a high degree of coupling between Mode I and Mode II stress intensity factors.

There are several ways to calculate the complex stress intensity factor K by solving the boundary value problem of the configuration within the realms of theory of elasticity.

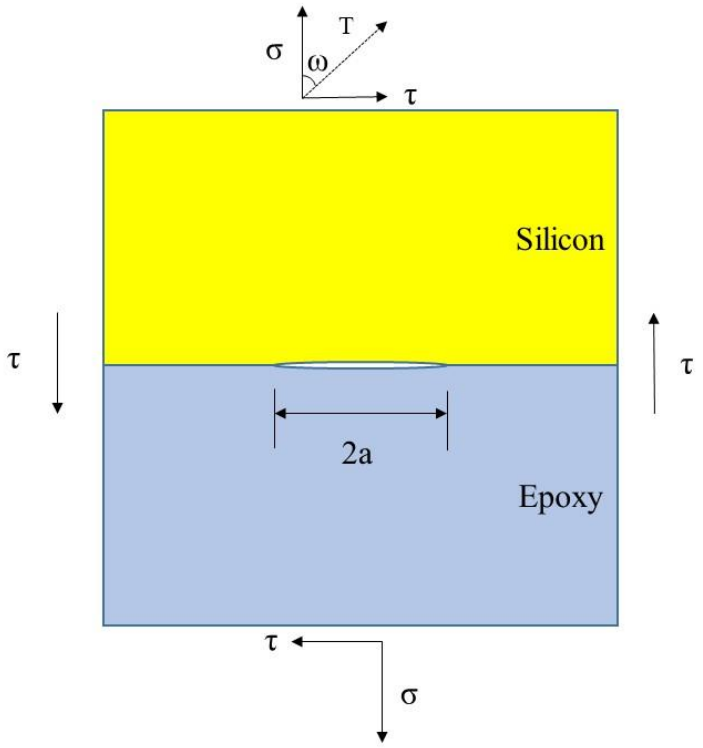

Figure 8: Bimaterial interface with an interface crack

Let's say a pre-existing crack of length 2a exists between the two semi-infinite material systems with remote tensile stress being σ and remote shear stress being τ in both materials. The transverse stresses however does not affect the stress intensity factor. Near the crack, both materials are in inhomogenous state. This boundary value problem has been solved by Rice and Sih [16]-

$$K = (1 + 2i\varepsilon)\sqrt{\pi a}(2a)^{-i\varepsilon}(\sigma + i\tau) \qquad (9)$$

Now we can express the remote load (T) as a function of its magnitude (σ) and direction (ω) as follows-

$$\sigma + i\tau = Te^{i\omega} \qquad (10)$$

So the stress intensity factor becomes

$$K = (1 + 2i\varepsilon)\sqrt{\pi a}(2a)^{-i\varepsilon}Te^{i\omega} \qquad (11)$$

The amplitude of the stress intensity factor is defined by

$$|K| = \sqrt{K\bar{K}} \qquad (12)$$

The real-valued quantity has the familiar dimension:

$$|K| = [\text{stress}][\text{length}]^{1/2} \qquad (13)$$

Indeed, $|K|$relates to the energy release rate G as [17]-

$$G = \frac{1}{2}\left(\frac{1}{E_1} + \frac{1}{E_2}\right)\frac{|K|^2}{\cosh^2(\pi\varepsilon)} \qquad (14)$$

Using these theoretical equations, a good understanding of crack behavior can be predicted. However, for very complex and nonlinear geometries a more accurate prediction can be made through the development of a finite element model that captures the irregularities in geometries as well viscoelastic or viscoplastic material properties. [18, 19 and 20] are some novel attempts on developing a simple elastic-plastic-creep finite element analysis (FEA) model including the various surface roughness features. The trick is to perform a two-tier modeling with the global model capturing the entire structure with all its far-field loading and then the local model capturing the crack tip behavior based on the near-field stresses. The exact material layers involved maybe different but similar modeling framework can also be developed for silicon-polymer interfaces.

Of course there are experimental ways to compliment this as well. Sandwich specimens can be developed to measure the fracture energy of an interface between a thin film of material 1 and a substrate of material 2. One can sandwich the film between two substrates of material 1 and use a layer of adhesive, such as epoxy to glue the bare substrate to the one covered with the film. The substrates are much thicker than the film and the adhesive, so the whole specimen is easy to load. The interfacial fracture energy can be measured if the crack runs on the desired interface. Another efficient way of measuring the interfacial fracture energy would be to perform a 4 point bend test.

A combination of any of these techniques can lead to a good measurement of the fracture energy. The following sections discusses how the crack growth rate and therefore the life estimation can be deduced from the stress intensity factor (or strain energy release rate) value.

Cyclic Environmental Conditions and Crack Growth Rates

As described in the previous section, the distribution of elastic stresses near the crack tip in an elastic body are described in terms of the stress intensity, K. With knowledge of this parameter, the elastic stress components can be estimated near the crack tip. However, plasticity does occur in a local region of the crack tip, as reflected in simplified diagram in Figure 9. The radius of the plastic region depends on the yield strength and may be approximated as shown in equation (15) [21].

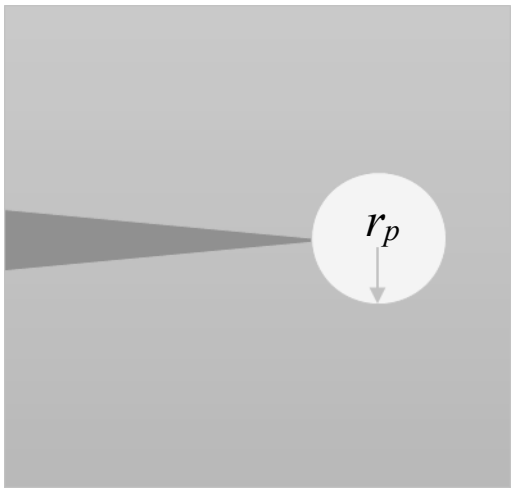

Figure 9: Simplified view of plastic region near the tip of a propagating crack.

Where r_p is the radius of the plastic zone and S_y is the yield strength.

$$r_p = \frac{1}{6\pi}\left[\frac{K}{S_y}\right]^2 \qquad (15)$$

Values for *K* can be calculated for different loading and geometric configurations from consideration of the theory of elasticity. In general , *K* has the units MPa $m^{1/2}$and takes the following form:

$$K = \psi \cdot S\sqrt{\pi a} \qquad (16)$$

where S is the nominal stress developed in the component under load and a is the crack length for an edge crack. ψ is a function of the ratio of the crack length, a, to the cross sectional width, W. W is the length that the crack must traverse to cause failure. Ψ depends on the geometry of the component. Deriving functional forms of K for complex, layered microelectronic package structures is a complex modeling task.

Under cycling conditions that induce stable fatigue crack growth, the stress range may defined as ΔS where $\Delta S = S_{max} - S_{min}$. Correspondingly, the stress intensity range becomes

$$\Delta K = \alpha \cdot \Delta S\sqrt{\pi a} \qquad (17)$$

The Paris Equation describes the rate of crack growth per loading cycle, $\frac{da}{dN}$, over the range of ΔS in terms of the stress intensity range, ΔK. This takes the form of equation (18)

$$\frac{da}{dN} = A \cdot [\Delta K]^m \qquad (18)$$

where *A and m* are constants and *m* is unique to a given material or interface.

It is often easier to estimate strain energy release, *G*, in testing basic materials or interface behavior. In this case the Paris equation takes the form:

$$\frac{da}{dN} = C \cdot [\Delta G]^n \qquad (19)$$

G is a function of K^2 depending upon geometry and materials.

Figure 10 shows the general behavior of crack growth in materials for components that undergo cyclic loading. Below a threshold stress intensity, ΔK_{th}, there is no crack growth; the crack remains quiescent. The linear *Paris region* is a region in which the Paris equation applies. This is a predictable and stable crack growth often termed sub-critical crack growth. Beyond this region, at the Fracture Toughness, *Kc*, crack growth is rapid and unstable. This behavior will be exhibited for each loading condition and crack opening mode reflected in Figure 6.

Given Mode I loading, with plane strain conditions, K_{Ic} is known as the Mode I fracture toughness or simply fracture toughness; it is most often characterized in testing for materials used in structural applications. Applying equation (16) under the condition $K = K_{Ic}$, allows for calculation of critical crack sizes, a, in which impending failure will occur in components under load. Predictions of life or cycles to

failure require the integration of equation (18) between an initial defect size and a critical crack size at which failure occurs.

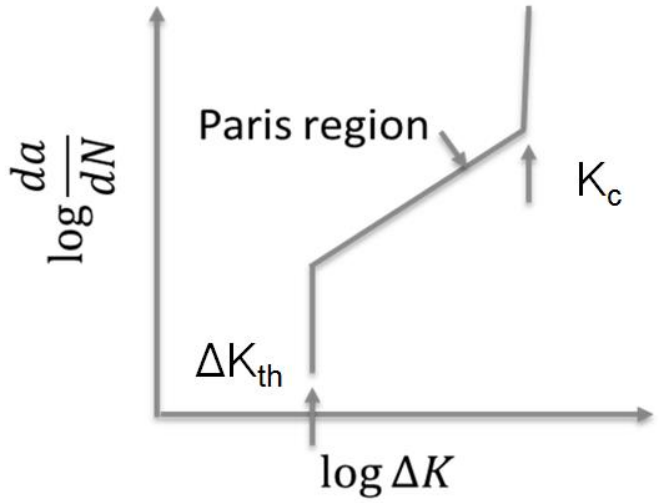

Figure *10:* Behavior of crack growth in materials under cyclic loading conditions. The Paris Equation applies over the linear region between the threshold and fracture toughness and extend over several orders of magnitude in crack growth.

Acceleration Factors for Delamination

While stress and subsequently life *prediction* is complex, a useful acceleration factor can be derived for crack growth and applied to thermal cycling conditions to support accelerated tests for microelectronic devices; acceleration factors deal with proportional quantities and not predictions. The Acceleration Factor, AF, in terms of the cycles, N, accumulated under test and use conditions, can be expressed as follows:

$$\mathrm{AF} = \frac{\mathrm{N_{use}}}{\mathrm{N_{test}}} \qquad (20)$$

Combining equations (17) and (18) and integrating for N:

$$\mathrm{N} = \frac{\mathrm{A}}{\Delta \mathrm{S}^{\mathrm{m}}} \cdot \frac{1}{\sqrt{\pi}} \int \frac{1}{\alpha \mathrm{a}^{1/2}} \mathrm{da} \qquad (21)$$

Since A, ψ, a and π are all constants, hence the following can be stated-

$$\mathrm{N} \propto \frac{1}{\Delta \mathrm{S}^{\mathrm{m}}} \qquad (22)$$

From equation (1) the nominal stress range is proportional to the temperature range of the temperature cycle when a body is undergoing temperature changes:

$$\Delta S \propto \Delta T \qquad (23)$$

Then it follows from equation (20) that for two different conditions, use and test:

$$AF = \frac{N_{use}}{N_{test}} = \left[\frac{\Delta T_{test}}{\Delta T_{use}}\right]^{m} \qquad (24)$$

When strain energy release rate is the primary consideration:

$$\Delta G \propto (\Delta K)^2 \qquad (25)$$

Then, given equations (1), (19) and (25), the AF is expressed as:

$$AF = \frac{N_{use}}{N_{test}} = \left[\frac{\Delta T_{test}}{\Delta T_{use}}\right]^{2n} \qquad (26)$$

To make these AF factors useful for thermal cycling tests of microelectronic devices, m or n must be known. These values may be extracted from controlled materials fracture tests with specialized specimen configurations that are conducted to characterize the material interfaces. A commonly used specimen is a double cantilever beam (DCB) from which the strain energy release rate and crack length during testing can readily be determined. It should be noted that these tests are normally isothermal. In addition, humidity can play a significant role in crack growth.

As an example of an isothermal crack growth test, Zhu et. al [22] tested a bilayer structure of a typical microelectronic polyimide film composition over SiN. The plot of the data are shown in Figure 11.

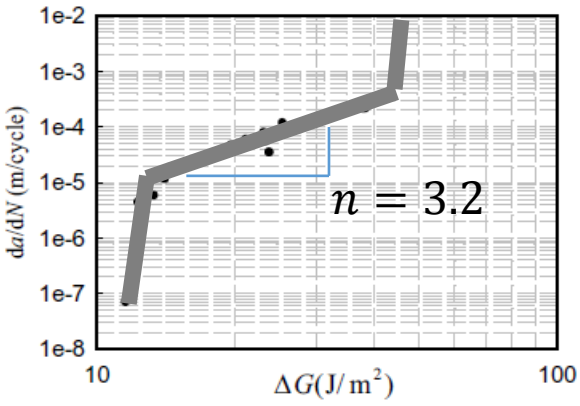

Figure 11: Strain Energy versus crack growth rate for polyimide over SiN using a DCB test. The data reflect a slope of n=3.2 in the stable crack growth regime. With permission of IEEE.

Applying equation (26), the acceleration factor AF is expressed as:

$$\mathrm{AF} = \frac{\mathrm{N_{use}}}{\mathrm{N_{test}}} = \left[\frac{\Delta \mathrm{T_{test}}}{\Delta \mathrm{T_{use}}}\right]^{6.4} \qquad (27)$$

Snodgrass et. al. [9] evaluated epoxy underfill to polyimide interfaces. Applying equation (19) resulted in a value of $n = 3.9$. For the materials tested, crack growth rates are apparently higher at the same energy release rate for the epoxy-polyimide interface then for the polyimide-SiN passivation layer interface. The acceleration factor for thermal cycling, derived as discussed is:

$$\mathrm{AF} = \frac{\mathrm{N_{use}}}{\mathrm{N_{test}}} = \left[\frac{\Delta \mathrm{T_{test}}}{\Delta \mathrm{T_{use}}}\right]^{7.8} \qquad (28)$$

The large value of the exponents indicates that life tests on actual microelectronic package elements can be conducted in a relatively short time, over temperature ranges compatible with polymers, to assure that crack propagation will not present a risk in the field. This is significant since crack propagation precedes other failure mechanisms. This also indicates some caution is warranted in selecting test temperature ranges for plastic encapsulated microelectronic devices to ensure that unrealistic *over acceleration* does not occur. This, in turn, may reflect the need for procedures that differ from ceramic enclosures for conducting qualification tests.

Table 1: Epoxy material on SiN under different loading conditions. (Courtesy of Reinhold Dauskardt, Stanford University)

Stress Ratio (R)	Slope (m)
0.5	6.8
0.3	7.7
0.1	8.1

Table 1 shows tests done for an epoxy material on SiN by the Dauskardt Group in Stanford University. R denotes the stress ratio for the tests [21].

$$\mathrm{R} = \frac{\mathrm{S_{min}}}{\mathrm{S_{max}}} \qquad (29)$$

A comparison of the slopes of the curves in the Paris region indicate similar behavior across the range of loading conditions with a relatively small trend.

Table 2: Benzocyclobutene (BCB) on SiO2 over different humidity ranges. (Courtesty of Reinhold Dauskardt, Stanford University.)

Humidity Level (RH)	Estimated Threshold Strain Energy Release Rate (J/m^2)	Slope (m)
1%	18.2	0.69
30%	23.2	0.34
40%	26.7	0.22
60%	34.3	0.21
90%	45.3	0.24

Table 2 shows tests conducted on Benzocyclobutene (BCB) -SiO_2, also by Dauskardt Group, over a range of humidity levels. It is clear that increasing humidity levels significantly shifts the threshold for which crack propagation is necessary for this system of materials. Further inspection also showed as the humidity levels increase above 40%, the slope of Paris region of these tests reflect very little change.

The strength and fracture properties of a bond depend upon the interphase layer thickness [5] and can be affected by aging and humidity depending on the hydrophilicity of the materials in the system [4]. The behaviors, reflected in Table 1 and 2, indicate that acceleration factors derived from DCB materials tests may have wide applicability over loading and environmental conditions due to relatively small changes in the slope *m* over a wide range of loading and environmental conditions.

Acceleration Factor for Polyimide Cracking

Notomi et. al. [23] also explored cracking of polyimide using a specialized type of small compact specimen and applying conventional crack propagation measurement methods. Compact specimen designs are often used for evaluating fracture behavior of bulk materials. Applying the Paris equation, they reported values for m for polyimide materials of varying molecular weight. They reported values of $3.3 < \mathrm{m} < 5.2$ and indicated crack growth rates decreased with increasing molecular weight.

Amagai [6] developed a model for life prediction of polyimide passivation coatings under specific conditions of an impinging plastic strain field on the polyimide coating due to the presence of a propagating delamination under temperature cycling. This model was developed for a specific type of

plastic package known as Small Outline J-Lead with Lead on Chip (LOC). The Amagai model was developed for a range of polyimide properties using simulation and Statistical Experimental Design.

The Amagai model, can be used to predict the number of cycles to produce a failing crack in a polyimide film, N. It is is expressed in terms of the nominal stress range developed in the polyimide, ΔS, in temperature cycling, the estimated radius of the plastic zone, r_p, at the delaminating crack tip, polyimide thickness, t, and polyimide film tensile toughness, Ω. Amagai applied finite element models for stress prediction.

The Amagai model is expressed as follows for the specific polyimide tested:

$$(\Delta S \cdot r_p)^{1.0985} \cdot N^{0.4497} = t \cdot \Omega \qquad (30)$$

While the model is derived for specific conditions, it yields a more general acceleration factor for cracking of polyimide film.

Given equation (20) and (30):

$$N^{0.4497} \propto \frac{1}{\Delta S^{1.095}}$$

$$N \propto \Delta S^{-0.2112} \qquad (31)$$

$$AF = \left(\frac{\Delta T_{Test}}{\Delta T_{Use}}\right)^{4.7}$$

The exponent derived for the acceleration factor based on the Amagai model for cracking of polyimide passivation in thermal cycling is within the range of values reported for isothermal fracture tests reported by Notomi et. al. [23]

Threshold Limits

The threshold temperature range at which crack propagation will occur is of considerable interest when designing accelerated tests to evaluate risks of defects contributing to failure. An estimate can be derived from simple considerations providing for a lower bound of concern for the threshold temperature range. As shown in Figure 8, crack propagation does not occur below a threshold stress intensity ΔK_{th}. Felck et. al [24] reported the lower bound of the Mode I threshold stress intensity for engineering polymers is approximately $\Delta K_{th} \geq 0.1$ MPa $m^{1/2}$. Fleck et. al [24] provided several plots of various materials to bound cyclic properties for design purposes; $\Delta K_{th}=0.1$ becomes a useful basis for estimating a threshold temperature range.

In evaluating a lower bound, a model for stress intensity is needed. For purposes of analysis of threshold limits herein, a block like structure under Mode II loading served as a closed form example for evaluating a lower bound of interest on the temperature range; the model for compact shear specimens was used for this purpose. The stress intensity for a compact shear specimen was explored in detail by Jones and Chisholm [25] and Hoyniak [26]. A symmetrical compact specimen with a driving stress, S, to deform the specimen and induce Mode II loading, has a closed form stress intensity shown in equations (32):

$$K = 1.1S\sqrt{\pi a} \qquad (32)$$

Considering thermal stresses as a driver, where delamination may occur between epoxy and a passivated silicon surface under cyclic loading, equation (1) can be applied as a first order approximation. Combining equation (1) and (32) yields the following:

$$\Delta K = 1.1 \cdot \bar{E}\Delta\alpha\Delta T \cdot \sqrt{\pi a} \qquad (33)$$

Considering a polymer in which the properties under mixed mode crack propagation are dominated by tensile behavior of the materials, and allowing $\Delta K = \Delta K_{th}$, the threshold ΔT for given crack sizes, a, can be estimated from equation (33).

As an example, polyimide passivated silicon die stack encapsulated in non-reinforced epoxy, with a potential for delamination between the polyimide and epoxy, is shown in Figure 12.

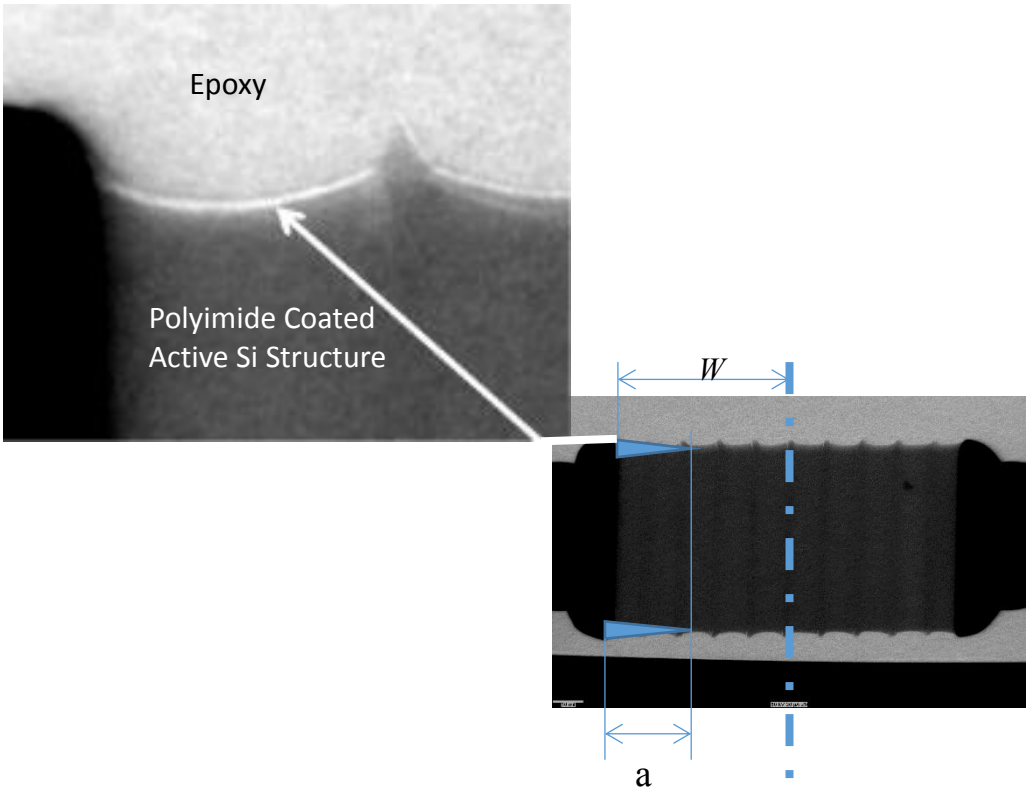

Figure 12: Polymide passivated die stack encapsulated in non-reinforced epoxy. Delamination of length, a, can be detected by radiographic inspection. (Radiography courtesy of Ahmed Amin, NASA GSFC.)

Considering that the stiffer elements drive stresses, the following approximations are made: $\Delta\alpha = \alpha_{\mathrm{epoxy}} - \alpha_{\mathrm{Si}}$ and $\overline{\mathrm{E}} = \mathrm{E}_{\mathrm{epoxy}}$; the threshold ΔT can then be evaluated for a delamination of length a, given $\Delta\mathrm{K}_{\mathrm{th}} = 0.1\ \mathrm{MPa\ m}^{1/2}$. Threshold $\Delta\mathrm{T}$ values are plotted against various crack sizes for the structure in Figure 13, under the assumptions stated.

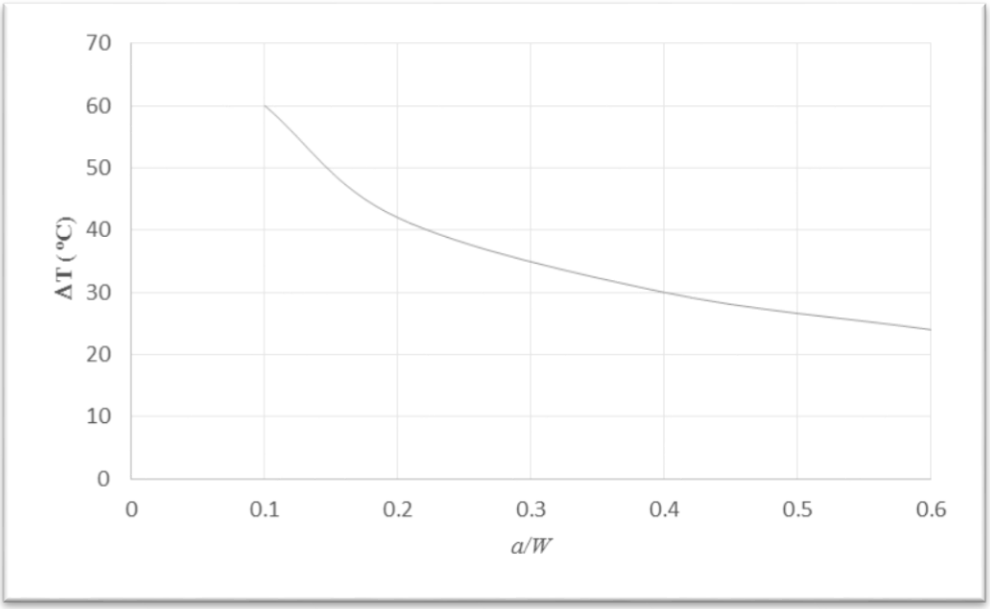

Figure 13: Estimated threshold ΔT at which delamination will grow, at the lower bound of threshold stress intensity for polymer materials, versus normalized crack length, for a block like silicon structure passivated with polyimide and encapsulated in unreinforced epoxy.

Figure 13 reflects for the simple structure that the threshold values of $\Delta\mathrm{T}$ necessary to propagate a delamination at $\Delta K_{th} = 0.1\ MPa\ m^{1/2}$ is relatively small and within the range of many typical thermal environments to which electronic products might be exposed. This lower bound estimate for the temperature range is also well below most test and screening environments.

Test Plans for Risk Informed Systems Qualification (RISQ)

Reliable and cost effective implementation of advanced packaging schemes is needed for most systems applications. This requires adequate testing and qualification strategies that can assure acceptable risks. Testing and qualification must be completed within schedule constraints to provide the necessary added value during development. The aforementioned acceleration factors can be used to facilitate this.

Risk Informed Systems Qualification (RISQ) can provide a cost effective approach to maximizing the information obtained from testing system packaging designs, and for qualification, as well as addressing potential risks from defects that might arise in a given assembly process. The approach for RISQ Analysis is outlined in Figure 14.

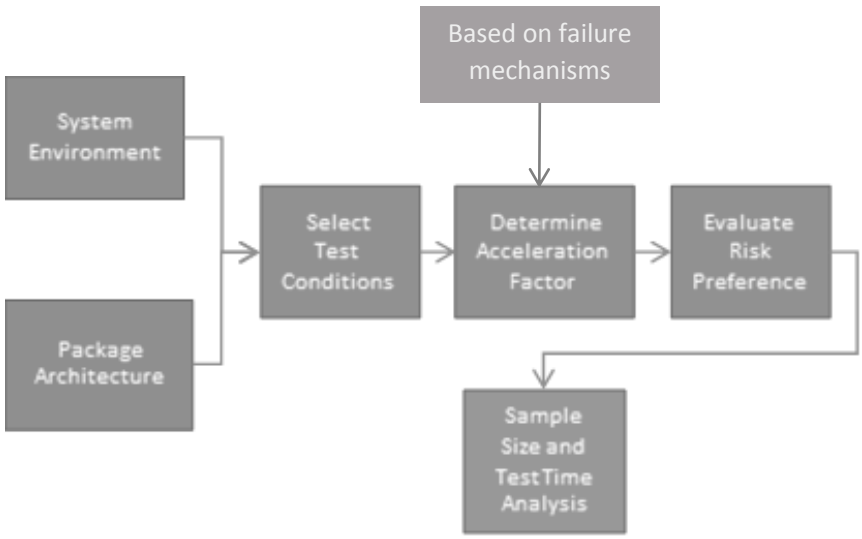

Figure 14: Risk Informed System Qualification (RISQ) Analysis process for developing accelerated testing for packaging.

System environments and selected architectures are inputs to the analysis. The environment encountered by the application will govern the appropriate selection of test conditions and models needed to develop acceleration factors [27, 28] appropriate to the failure mechanism and test design. The architectures selected are important, as materials systems and potential defect types are also important considerations in testing and test condition selection.

The conditions in which an assembly will be used depend upon several design factors of the system, as well as the external environment. Under the hood automotive environment may be substantially different from the cabin environment and for spacecraft, relevant system factors may include the position in which

the assembly is located on an orbiting vehicle, the size of the spacecraft, or the potential use of thermal controls.

Qualification testing often cannot be run in a reasonable time frame to demonstrate actual desired reliabilities of devices. However, tests may be run to a set of risk preferences for a given project. Risk preferences for a given system design are held by the decision maker. However, these may be influenced by standardized organizational risk preferences. An example of risk likelihood classification is shown in Table 3 for unmanned spacecraft. As comparison, in automotive applications, the preferred test may be to demonstrate a probability of failure, p, less than or equal to 0.1 at a confidence level, CL, equal to 95%.

Table 3: Risk Likelihood Classifications Used in GSFC-STD-0002 [29]. Prescribed probabilities of failure for classification of safety events and technical or performance risks are shown.

Likelihood	Safety (Estimated likelihood of safety event occurrence)	Technical (Estimated likelihood of not meeting performance requirements)
5 Very High	($P_{SE} > 10^{-1}$)	($P_T > 50\%$)
4 High	($10^{-2} < P_{SE} \leq 10^{-1}$)	($25\% < P_T \leq 50\%$)
3 Moderate	($10^{-3} < P_{SE} \leq 10^{-2}$)	($15\% < P_T \leq 25\%$)
2 Low	($10^{-6} < P_{SE} \leq 10^{-3}$)	($2\% < P_T \leq 15\%$)
1 Very Low	($P_{SE} \leq 10^{-6}$)	($0.1\% < P_T \leq 2\%$)

Using standardized risk preferences for qualification test design quickly informs projects concerning the impact of using new and advanced packaging technologies. In Table 3, p_{SE} denotes probability of failure for safety event and p_T denotes probability of failure for precipitating loss of performance.

Test scenarios can be developed using the well-known Binomial-Parametric Test design recommended by Kececioglu [30]. For this type of design, the desired component reliability to be demonstrated may be estimated from the Weibull distribution. The probability of passing the test at a given confidence is estimated from the Binomial Distribution. Hence, for a given sample size, *z*, the following model may be used:

$$1 - \mathrm{CL} = \sum_{k=0}^{r} \binom{z}{k} \left[1 - e^{\left(N_R/\eta\right)^{\beta}}\right]^{k} \left[e^{\left(N_R/\eta\right)^{\beta}}\right]^{z-k} \qquad (34)$$

where $\eta = \frac{N_{Use}}{(-\ln R(N)_{Demo})^{\frac{1}{\beta}}}$

In the above model, CL is the confidence limit, z is the number of samples, r is the allowable number of failures, N_R is the calculated number of cycles to be executed in test, without acceleration, to meet the required risk preference. β is the Weibull shape factor and N_{use} is the required field life. $R(N)_{Demo}$ is the reliability to be demonstrated in the test as determined from the risk preferences for the organization or project where:

$$R(N)_{Demo} = 1 - p \qquad (35)$$

where p is the risk preference or tolerable likelihood of occurrence of an undesirable event.

The *AF* can be redefined in terms of our RISQ process model as:

$$AF = \frac{N_R}{N_{Test}} = \left[\frac{\Delta T_{test}}{\Delta T_{use}}\right]^{m} \qquad (36)$$

Using Equations (34), (35) and (36), the CL, z, and N_{Test} can be traded off against each other for a fixed set of targets, N_{Use} and $R(N)_{Demo,}$ given a value for m. The value of m represents the failure mechanism the test is designed against. Finally, unless the test population is very large r=0.

It is very useful to present an example in applying the RISQ process. In this case, an example of a cubesat application for low cost spaceflight is shown. Cubesats will normally employ plastic encapsulated microcircuits given cubesat cost, power, mass and performance requirements. Considering a low Earth orbit (LEO), the expected temperature variation for an internal printed wiring assembly in a small cubesat structure may be as significant as – 20°C to +30°C or, ΔT=50°C, with each orbit [31]. However, this will ultimately depend on the thermal design. While many cubesats are designed for short life, the expectation is to expand their capability, mission and lifetime. A 3-year mission life in LEO will require 17,520 cycles.

In order to apply the RISQ process model for developing qualification schemes for the plastic packages for the cubesat example, the Weibull slope for failure due to crack growth in the polymers is needed. Rusanen and Lenkkeri [32] determined that the Weibull shape parameter for fracture of epoxy polymer flip chip bumps was $1.4 \leq \beta \leq 2.5$. This range values may be similar to the expected Weibull shape parameter for fracture and crack propagation in polymer packages where failure is defined to be a crack of sufficient size to result in activating another failure mechanism or precipitating the expected failure mode.

Selection of test conditions should be judiciously made in view of the principles of fracture mechanics of polymers. Unless sophisticated analytical modeling techniques are employed to interpret the test results, the maximum test temperature should not exceed the glass transition temperature. The CTE and modulus

of the polymers will dramatically change at this temperature, as the polymer undergoes a phase change. For application in which moisture and humidity is an operational consideration, the maximum temperature change can be kept below 100°C. This will afford the ability to control humidity levels during the test. In addition, elevated humidity may favor crack propagation and lower threshold stress intensities, K_{th}. For the cubesat example, the operational and test conditions selected are shown in Table 4.

Table 4: Operational and Test Conditions for a Cubesat Application

Operational and Test Parameters	Range or Value
Maximum Orbital Temp Range (°C)	-40 to +80
Device Max Operating Limits (°C)	-40 to +100
Payload Operating Range (°C)	-10 to +40
Operational Cycle (mins)	90
Payload Design Life (years)	3
Payload Design Life (cycles)	17520
Life Test Temp Range (°C)	-40 to +80
Half Cycle Hold Time (mins)	15
Humidity Control (%RH)	None
Delamination Acceleration Factor (m=7.8)	923
Polyimide Cracking Acceleration Factor (m=4.7)	61

Table 5: Test Options for Cubesat Microelectronic Qualification

for Delamination and Cracking in Polymers

Thermocycling -40°C to +80°C for 3 Year Mission Life

Sample Size, z	5	10	15
Allowed Failures, r	0	0	0
Weibull Shape Parameter, β	1.4	1.4	1.4
Confidence Level , CL	90%	90%	90%

Demonstrated Reliability , $R(N)_{Demo}$	0.98	0.98	0.98
Life at Reliability Level, N_{Field} (cycles)	17520	17520	17520
Required Failure Free Test Time, N_R (cycles)	163462	99631	74579
Delamination Epoxy-Polyimide Interface, N_{test} (cycles)	177	108	81
Polyimide Passivation Cracking, N_{test} (cycles)	2680	1633	1223

Options for a RISQ based life test qualification plan for plastic microcircuits are reflected in Table 5 for a risk preference of p=2%, which is the maximum allowable accepted likelihood for a failure event, in which safety is not the prime consideration, to remain in a very low risk regime.

Table 5 reflects the large acceleration factors for delamination of the epoxy-polyimide interfaces for the qualification test design. This does not infer that the plastics are not capable of meeting the application requirement. It reflects the sensitivity of a propagating crack or delamination to the cyclic load. It can be expected, given this sensitivity, that defects would rapidly manifest themselves as growing cracks during thermal cycling. However, from experience, some satisfactorily processed plastic encapsulated devices can survive and provide electrical performance after severe thermal shock from -55^{o}C to +125^{o}C [33]. However, such tests are not necessarily quantitative. Testing, if not appropriately applied, may limit the range of packaging technologies that can successfully meet requirements of the application.

In applying acceleration factors, it is important not to extend the test conditions beyond the model's limits to explain the materials behavior. In general, for polymers subject to cyclic loading, it is best to select test designs in which the applied stresses are such that $N_{Test} \geq 10^2$ cycles and $N_{use} \leq 10^6$ cycles. Acceleration factors which project significantly outside this range may not be accurate. Fatigue behavior should not be expected to be linear outside these bounds [34].

Since polymer failure is precursor to electrical failure, the devices under test must be inspected following the test. Qualification or life test runs should include periodic electrical functional tests, radiography, scanning acoustic microscopy, or destructive analysis to evaluate the devices as test cycles are accumulated.

Conclusions

The reliability of plastic encapsulated microelectronics depends upon the integrity of the polymers, primarily epoxies and polyimides, which enclose and protect the devices. Effective quantitative accelerated life testing must include consideration of the failure of these polymer constituents and their respective interfaces. This is achieved through consideration of the failure mechanism, crack propagation and growth, that dominate these materials and precedes electrical failures and other mechanical fatigue processes. The principles of Linear Elastic Fracture Mechanics (LEFM) have been shown to effectively describe these processes in polymers.

The application of fracture mechanics, including the Paris Equation, yields quantitative, yet simple, acceleration factors of familiar form that can be used to bound appropriate quantitative accelerated life tests for microelectronic parts. These tests can demonstrate effective risk reduction to real systems where the parts are employed. The parameters of these factors can be extracted from fracture tests that directly characterize the materials used in the encapsulation of microelectronics. Furthermore, application of

LEFM reveals the sensitivity of crack growth in polymers to stresses, which can be capitalized on to build appropriate and reasonable quantitative testing schemes.

Acknowledgement

The author wish to acknowledge the support of NASA for completion of this work.

References

[1] Puttlitz, K.J. and Totta, P. A., edts, Area Array Interconnection Handbook, Springer, (2001).

[2] Benson, R.C., Farrar, D., and Miragliotta, J., Polymer Adhesives and Encapsulants for Microelectronic Applications, Johns Hopkins APL Technical Digest, Volume 28, Number 1 (2008), pp 58-71.

[3] Evans J.,and Evans, J., Electronic Materials and Properties, Electronic Packaging Handbook, Marcel Dekker, (1991).

[4] Luo, Shijian and Wong, C.P., Influence of Temperature and Humidity on Adhesion of Underfills for Flip Chip Packaging, IEEE Transactions on Components and Packaging Technologies, Vol. 28, No. 1, (2005), pp 88-94.

[5] Hoontrakul, P., Sperling, L.H., Pearson, R.H., Understanding the Strength of Epoxy-Polyimide Interfaces for Flip-Chip Packages, IEEE Transactions on Device and Materials Reliability, Vol. 3, No. 4. Dec. (2003), pp 159-*166.*

[6] Amagai, M., Polyimide Fatigue Induced Chip Surface Damage in DRAM Lead on Chip (LOC) Packages, Proceedings of International Reliability Physics Symposium, IEEE, April (1995), Las Vegas, NV, pp 97-106.

[7] Matsubara, G., Ono, H., Tanaka, K., Mode II fatigue crack growth from delamination in unidirectional tape and satin-woven fabric laminates of high strength GFRP, International Journal of Fatigue 28 (2006), pp 1177-1186.

[8] Zhang, Y.L., Shi, D .X.Q., Zhou, W., Reliability study of underfill/chip interface under accelerated temperature cycling (ATC) loading, Microelectronics Reliability, 24, (2006), pp 409-420.

[9] Snodgrass, J.M., Pantelidis, D., Bravman, J.C. and Dauskardt, R.H., The Effects of Environment and Fatigue on the Adhesion and Subcritical Debonding of Dielectric Polymers, Proc. of the MRS, Janurary, (1999), pp 123-128.

[10] Kook, S.Y. and Dauskardt, R.H, Moisture-assisted subcritical debonding of a polymer-metal interface, Journal OF Applied Physics, Vol. 91, No. 31, Feb, (2002), pp 1293-1302.

[11] Giachino, M., Dubois,G. and Dauskardt, R. H., Molecular Design for Moisture Insensitivity of Compositionally Graded Hybrid Films, ACS Appl. Mater. Interfaces, Vol. 7, Issue 12, March, (2015), pp 6812-6818.

[12] Sharratt , B.M.,, Wang, L.C., Dauskardt, R.H, “Anomalous debonding behavior of a polymer/inorganic interface , Acta Materialia, Vol. 55 , 2007, pp 3601–3609.

[13] O’Brien, T. K, Composite Interlaminar Shear Fracture Toughness G_{IIc}: Shear Measurement or Sheer Myth, NASA Technical Memorandum, NASA TM 110280, February, (1997).

[14] V. L. Hein and F. Erdogan, “Stress singularities in a two-material wedge”, International Journal of Fracture Mechanics, Vol. 7, (1971), pp. 317-330.

[15] M. L. Williams, “The stresses around a fault or crack in dissimilar media”, Bull. Seismological Soc. Amer., Vol. 49, (1959), pp. 199-204.

[16] J. R. Rice and G. C. Sih, “Plane problems of cracks in dissimilar media”, Journal of Applied Mechanics, Vol. 32, (1965), pp. 418-423.

[17] B. M. Malyshev and R. L. Salganik, “The strength of adhesive joints using the theory of crack”, International Journal of Fracture Mechanics, Vol. 1, (1965), pp. 114-128.

[18] K. Sinha, J. Varghese and A. Dasgupta, Effect of geometric complexities and nonlinear material properties on interfacial crack behavior in electronic devices, Microelectronics Reliability, Vol. 54, Issue 3, (2014), pp. 610-618.

[19] K. Sinha, “Mechanics of Nonplanar Interfaces in Flip-Chip Interconnects”, PhD Thesis, University of Maryland, College Park, Maryland, (2012).

[20] K. Sinha, D. Farley, T. Kahnert, S. D. Solares, A. Dasgupta, J.F.J. Caers and X. J. Zhao, Influence of fabrication parameters on bond strength of adhesively bonded flip-chip interconnects, Vol. 28, Issue 12, (2014), pp. 1167-1191.

[21] Fuchs, H.O. and Stevens, R. I., Metal Fatigue in Engineering, John Wiley and Sons, (1980).

[22] Zhu, S.W., Shih, C.P., Chiu, T.C., Shen, G.S., Delamination Fracture Characteristics for Polyimide Related Interfaces under Fatigue Loading, 5th International Microsystems Packaging Assembly and Circuits Technology Conference (IMPACT), October (2010), Taipei, Taiwan, pp 1-4.

[23] Notomi, M., Kishimoto, K., Shibuya T., Inaba, H. and Morita, A., Discontinuous Crack Growth of Polyimide Resin, Effect of Molecular Weight, Tran. Jap. Soc. Mech. Engineers, A, Vol. 65, No. 629, (1999), pp 67-71.

[24] Fleck, N. A.; Kang, K. J.; Ashby, M. F., Overview No. 112: The cyclic properties of engineering materials, Acta metal. Mater. Vol. 42, No. 2, pp 365-381, (1994).

[25] Jones, D.L. and Chisholm, D.E., An Investigation of the edge sliding mode in fracture mechanics, Engineering Fracture Mechanics, Vol. 7, (1975), pp 261-270.

[26] Hoyniak, D., Parametric Study of a Compact Shear Fracture Specimen by Finite Element Techniques, Naval Sea Systems Command, TM -76-196, August, (1976).

[27] S. Ganesan, V. Eveloy, D. Das, M. Pecht, Identification and utilization of failure mechanisms to enhance FMEA and FMECA, Proc. IEEE Workshop Accel. Stress Test. Reliab. (ASTR), Austin, TX, Oct 3-5 (2005).

[28] J. Hu, D. Barke, A. Dasgupta, A. Arora, Role of failure-mechanism identification in accelerated testing, J. IES, 36(4) (1993), pp. 39-45.

[29] GSFC-STD-0002, Risk Management Reporting, (2009).

[30] Kececioglu, D. K., Reliability and Life Testing handbook, Vol. 1, Prentice-Hall, (1993).

[31] Reiss, P., Hager, P., Macdonald, M., and Lucking, C., New Methodologies for the Thermal Modelling of CUBESATS, 26th Annual AIAA/USU Conference on Small Satellites, Aug, (2012).

[32] Rusanen, O., and Lenkkeri, J., Thermal Stress Induced Failures in Adhesive Flip Chip Joints, The International Journal of Microcircuits and Electronic Packaging, Volume 22, Number 4, Fourth Quarter, (1999), pp 363-369.

[33] Thompson, P., Koehler, C., Petras, M., Solis, C., Flip-Chip BGA Assembly Process and Reliability Improvements, Proc. of International Electronics Manufacturing Technology Symposium, IEEE, Oct (1996), Austin, TX, pp 84-90.

[34] Meyers, M. A. and Chawla, K.K., Mechanical Behavior of Materials, 2nd Edition, Cambridge University Press, (2009).

[35] Suhir, E., Flip-Chip Assembly: Is the Bi-Material Model Acceptable?, J Mater Sci: Mater Electron (2017). https://doi.org/10.1007/s10854-017-7471-8

[36] Suhir, E., An Approximate Analysis of Stresses in Multilayered Elastic Films, Transactions of the ASME Journal of Applied Mechanics, Volume 55, No. 143, March (1988)